Hedi Soussi,[1,2,3] Sophie Reggio,[1,2,3] Rohia Alili,[1,2,3] Cecilia Prado,[2] Sonia Mutel,[1,2,3] Maria Pini,[1,2,3] Christine Rouault,[1,2,3] Karine Clément,[1,2,3] and Isabelle Dugail[1,2,3]

DAPK2 Downregulation Associates With Attenuated Adipocyte Autophagic Clearance in Human Obesity

Diabetes 2015;64:3452–3463 | DOI: 10.2337/db14-1933

OBESITY STUDIES

Adipose tissue dysfunction in obesity has been linked to low-grade inflammation causing insulin resistance. Transcriptomic studies have identified death-associated protein kinase 2 (DAPK2) among the most strongly downregulated adipose tissue genes in human obesity, but the role of this kinase is unknown. We show that mature adipocytes rather than the stromal vascular cells in adipose tissue mainly expressed DAPK2 and that DAPK2 mRNA in obese patients gradually recovered after bariatric surgery–induced weight loss. DAPK2 mRNA is also downregulated in high-fat diet–induced obese mice. Adenoviral-mediated DAPK2 overexpression in 3T3-L1 adipocytes did not affect lipid droplet size or cell viability but did increase autophagic clearance in nutrient-rich conditions, dependent on protein kinase activity. Conversely, DAPK2 inhibition in human preadipocytes by small interfering RNA decreased LC3-II accumulation rates with lysosome inhibitors. This led us to assess autophagic clearance in adipocytes freshly isolated from subcutaneous adipose tissue of obese patients. Severe reduction in autophagic flux was observed in obese adipocytes compared with control adipocytes, inversely correlated to fat cell lipids. After bariatric surgery, adipocyte autophagic clearance partially recovered proportional to the extent of fat cell size reduction. This study links adipocyte expression of an autophagy-regulating kinase, lysosome-mediated clearance and fat cell lipid accumulation; it demonstrates obesity-related attenuated autophagy in adipocytes, and identifies DAPK2 dependence in this regulation.

Adipose tissue function includes the deposition of nutrient-derived energy excess as lipids and the integration of energy balance signals to produce leptin and adiponectin required for metabolic homeostasis. Chronic energy balance disruption as seen in obesity leads to adipose tissue lipid overload and adaptive stress responses toward ultimate dysfunction and metabolic inflexibility (1). Large-scale transcriptomic studies of adipose tissue from obese patients or obese rodent models pointed to inflammatory pathways as a prominent response to lipid overload (2–4). Inflammation in obesity results from tissue remodeling by immune cell infiltration/proliferation within the adipose fat depot (5). Indeed, whereas the adipocyte is the predominant cell type in healthy lean adipose tissue, immune cells can equal or even exceed fat cell number in obesity. Metabolic inflammation is now recognized as a key factor in obesity-related insulin resistance and the subject of current investigations of immune cell subpopulations (6) toward novel therapeutic approaches.

Besides identification of expression networks and associated biological functions, transcriptomic approaches also bring attention to single genes unrelated to annotated pathways. In the current study, we focus on death-associated protein kinase 2 (DAPK2), also called DRP-1, which hits among the most downregulated genes of the adipose tissue transcriptome in human morbid obesity (7). DAPK2 belongs to a family of serine/threonine calmodulin-regulated protein kinases that consists of five members, all displaying high sequence homology in their N-terminal kinase domains, whereas COOH-terminal regions highly diverge. DAPK1, the founding family member, is involved in apoptosis (8) and is suppressed in many tumors (9). Unlike DAPK1, DAPK2 and other DAPKs are devoid of a COOH-terminal death domain, ankyrin repeats, and

[1]Nutriomics Team, INSERM, UMR_S U1166, Paris, France
[2]Université Pierre et Marie Curie, Sorbonne Universités, UMR_S 1166, Paris, France
[3]Institute of Cardiometabolism and Nutrition, Assistance Publique-Hôpitaux de Paris, Pitié-Salpêtrière Hospital, Paris, France
Corresponding author: Isabelle Dugail, isabelle.dugail@inserm.fr.

Received 23 December 2014 and accepted 21 May 2015.
This article contains Supplementary Data online at http://diabetes.diabetesjournals.org/lookup/suppl/doi:10.2337/db14-1933/-/DC1.

cytoskeleton-interacting region (9). Therefore, DAPK2 is a small protein that only contains a kinase domain, a calmodulin binding region, and a short tail with undefined structural motifs. DAPK2 is ubiquitously expressed, but its physiological functions are still largely unknown. Interestingly, large-scale RNA interference kinome screens identified DAPK2, suggesting a role in autophagy (10), secretory pathway (11), or transforming growth factor-β signaling by protein-to-protein interaction (12).

In the current study, we investigated the significance of DAPK2 downregulation in human obesity. We first identified adipocytes and not other nonlipid filled adipose tissue cells as targets of DAPK2 downregulation. Then, the effects of DAPK2 gain/loss of function in cultured adipose cells revealed a regulatory role of the kinase in lysosome-mediated remodeling, which led us to further investigate adipocyte autophagic clearance in human obesity and weight loss. We demonstrated attenuation of adipocyte autophagic activity in human obesity, partially reversible after weight loss after bariatric surgery. Thus, these results link DAPK2 downregulation and defective autophagy to fat cell dysfunction in human obesity.

RESEARCH DESIGN AND METHODS

Human Adipose Tissue Samples

All subjects gave their informed consent in an accepted protocol related to the physiopathology of obesity (Assistance Publique-Hôpitaux de Paris, Clinical Research Contract). Clinical investigations were performed according to the Declaration of Helsinki and approved by local ethics committees. Middle-aged obese subjects who were candidates for bariatric surgery were not on a restrictive diet and their weights were reported stable. All subjects met usual eligibility criteria for bariatric surgery. Follow-up of patients after gastric bypass included monitoring of weight loss and obtaining subcutaneous adipose tissue biopsy specimens from the abdominal region. All tissue samples were processed immediately for adipocyte isolation or frozen for mRNA extraction.

Control subjects were nonobese subjects undergoing plastic surgery or planned surgery for gall bladder ablation or hernia. None had diabetes or metabolic disorders or were taking medication. Main characteristics of the patient groups are summarized in Table 1.

Adipocyte Isolation

Floating adipocytes were obtained by collagenase digestion essentially as described by Rodbell (13), except that DMEM was used instead of Krebs-Ringer buffer. Floating adipocytes were separated from the stromal vascular fraction (SVF) cells by aspirating the infranatant and rinsing three times with DMEM. Minor contamination of the adipocyte fraction by stromal vascular cells was checked on morphological images of adipocyte suspensions used for fat cell size determination.

Cell Culture

3T3-L1 cells were maintained and differentiated in standard conditions. Adenovirus was obtained by recombination of viral backbones with shuttle vectors containing DAPK2 cDNAs and packaging in complementing 293 cells, as described previously (14). GFP-LC3 3T3-L1 stable transfectants were obtained as described (15). Human preadipocytes were isolated from subcutaneous adipose tissue and cultured as described (16). Small interfering (si)RNA–mediated knockdown was performed with 20 nmol/L siRNAs using lipofectamine RNAiMAX (Invitrogen) according to the manufacturer's instruction. DAPK2 siRNA sequence was from Abgent (5′-UGUCU GGAGGAGAGCUCUUTTAAGAGCUCUCCUCCAGACATT-3′). Scrambled siRNAs were used as controls. Fresh medium supplemented with antibiotics and 10% SVF was added 16 h after transfection, and cells were incubated for a further 24 h.

Mice Studies

Male *ob*/*ob* and *ob*/+ mice were maintained on a normal chow diet with ad libitum feeding and killed at 12–16 weeks of age (body weights 30.1 ± 3.1 vs. 58.2 ± 3.4 g). C57BL/6J male mice were fed a high-fat diet (60% calories from fat) for 16 weeks from weaning onward and killed (body weights 37.9 ± 1.8 vs. 48.2 ± 3.5 g).

mRNA Quantification

mRNAs were reversed transcribed and cDNA were quantified by real-time RT-PCR using qPCR MasterMix Plus for SYBR Green (Eurogentec). The PCR efficiency of primer pairs was checked in standard curves, and expression data were expressed using the ΔΔCt method. 18S RNA was used for normalization. The sequence of primer pairs for DAPKs was as follows:

Human DAPK2: 5′-ACGTGGTGCTCATCCTTGA-3′ and 5′-TGGCCTCCTCCTCACTCA-3′.
Mouse DAPK2: 5′-GACGTGGTGCTCATCCTTG-3′ and 5′-GGCTTCCTCCTCACTTAACGA- 3′.
Mouse DAPK1: 5′-CCTGATTTCCAGGACAAGG-3′ and 5′-CTTTAGCCACGGAGTAATCAGCC-3′.
Mouse DAPK3: 5′-ATTTGTACCGGAGGTTCTCG-3′ and 5′- TCTGAAGGATTCTGGGGACA-3′.

A complete list of the other primer sequences is provided in the Supplementary Data.

Autophagic Flux Measurement

Experimental design followed state of the art guidelines (17). Freshly isolated floating adipocytes or differentiated cells lines were rinsed with high-glucose DMEM and incubated for 2 h in the presence of 100 nmol/L bafilomycin A1, 100 μmol/L leupeptin/20 mmol/L NH_4Cl, or 25 μmol/L chloroquine at 37°C in a humidified 95% air/5% CO_2 atmosphere. Cells were collected in lysis buffer (50 mmol/L Tris [pH 7.4], 0.27 mol/L sucrose, 1 mmol/L Na-orthovanadate, 1 mmol/L EDTA, 1 mmol/L EGTA, 10 mmol/L Na β-glycerophosphate, 50 mmol/L NaF, 5 mmol/L Na pyrophosphate, 1% [w/v] Triton X-100, and 0.1% [v/v] 2-mercapto ethanol) supplemented with Complete protease inhibitors and stored frozen at −20°C before further processing.

Table 1—Description of patients

	Lean (n = 22)	Overweight (n = 10)	Obese (n = 65)	Obese (for surgery follow-up) (n = 9)
Sex, *n*				
Female	20	4	38	9
Male	2	6	27	0
BMI (kg/m^2)	23.6 ± 3.2	26.35 ± 0.19	47.56 ± 0.04	42.55 ± 3.14
Age (years)	38 ± 11	43 ± 2	47 ± 0.05	33 ± 8
Subcutaneous fat cell diameter (μm)	87.4 ± 12	—	121.16 ± 0.04	119.9 ± 3.8

Data are presented as mean ± SEM unless indicated otherwise.

Western Blotting

Cell lysates were processed as previously described (18). Commercial antibodies against LC3, Akt, and β-actin were from Cell Signaling Technology, DAPK2 from ProSci, and p62 from Progen.

Lipolysis

Lipolytic rates were assessed in cells maintained for 2 h in phenol-red free medium containing 2% BSA with or without 10^{-5} mol/L isoproterenol for lipolytic stimulation. Glycerol release was measured using a glycerol colorimetric assay kit (Cayman Chemical, Ann Arbor, MI) and normalized to cell protein content.

Cell Imaging

3T3-L1 stable transfectants expressing GFP-LC3 were differentiated and processed for fluorescent imaging as previously described (19). Intracellular lipid droplets and floating adipocytes were sized using Perfect Image (Clara Vision) from phase-contrast images. Immunofluorescence on paraffin-embedded adipose tissue sections was performed as described (20).

Statistical Analysis

Results are expressed as mean ± SEM. The Mann-Whitney *U* test was used in all analyses except for paired data, which were tested with the Wilcoxon signed rank test or the paired Student *t* test. The Spearman rank correlation test was used for correlations.

RESULTS

Downregulation of Adipocyte DAPK2 Expression in Human Obesity

Our attention on DAPK2 was brought by pangenomic transcriptome analysis comparing adipose tissue gene expression in lean and obese subjects (7). We confirmed a threefold decrease in DAPK2 mRNA (Fig. 1*A*) in subcutaneous adipose tissue samples from 65 severely obese (BMI range 34–79 kg/m^2) compared with 10 nonobese subjects (BMI range 20–23 kg/m^2), not influenced by type 2 diabetes (Fig. 1*B*) or by sex (not shown). Low DAPK2 mRNA expression was also independently confirmed in a subgroup of 24 severely obese compared with 10 overweight (BMI 24–28 kg/m^2) subjects (Fig. 1*C*), pointing to DAPK2 downregulation as a feature of severe obesity but not of simple overweight. Relative DAPK2 mRNA levels in obese subjects positively correlated with HDL cholesterol and inversely associated with triglyceridemia and serum interleukin 6 (IL-6). A trend for negative association to subcutaneous fat cell size (P = 0.057) was also observed (Table 2).

Because bariatric surgery (i.e., gastric bypass) is the most efficient intervention to induce weight loss in morbid obesity, we examined DAPK2 mRNA in 10 patients over time at 0, 3, 6, and 12 months after surgery. Gradual time-dependent recovery, almost complete after 12 months (Fig. 1*D*), indicated that DAPK2 loss was not irreversible in obese adipose tissue. We also found decreased DAPK2 mRNA in the subcutaneous adipose tissue of mice with diet-induced obesity, indicating common obesity-related DAPK2 regulation in humans and rodents (Fig. 1*E*). Adipose tissue digestion by collagenase was performed to determine relative DAPK2 mRNA expression in the isolated adipocyte and the nonlipid-filled stromal vascular cell compartment of human fat tissue. In nonobese as well as in obese subjects, DAPK2 mRNA was more abundant in adipocytes than in stromal vascular cells (Fig. 1*F*), and a major reduction with obesity was found in the adipocyte fraction (Fig. 1*F*). Thus, adipocyte-enriched DAPK2 expression is suppressed in human obesity and reversibly recovers after bariatric surgery–induced weight loss in humans. Immunofluorescence labeling of adipose tissue sections confirmed adipocyte DAPK2 suppression in obese patients at the protein level (Fig. 1*G*).

DAPK2 Modulates Lysosome-Mediated Remodeling and Constitutive Autophagy in Adipocytes

The bulk of human fat cells are renewed every 10 years, consistent with function in long-term energy storage, and the adipocyte is considered a long-lived cell type (21). In this context, the conserved process of intracellular organelle remodeling by lysosomes (i.e., autophagy) is crucial to maintain homeostasis (22), especially in oxidatively prone conditions linked to a lipid-rich adipocyte environment. Because DAPK2 was suggested as a potential autophagy regulator (10,23,24), we focused on constitutive autophagy in the presence of nutrients. We generated 3T3-L1 adipocytes stably expressing GFP-LC3, which retained full differentiation capabilities, as judged by the presence of large multilocular cytoplasmic lipid droplets. Fluorescent GFP-LC3 distribution identified autophagosome vesicles, visualized as punctuated labeled structures (Fig. 2*A*) and

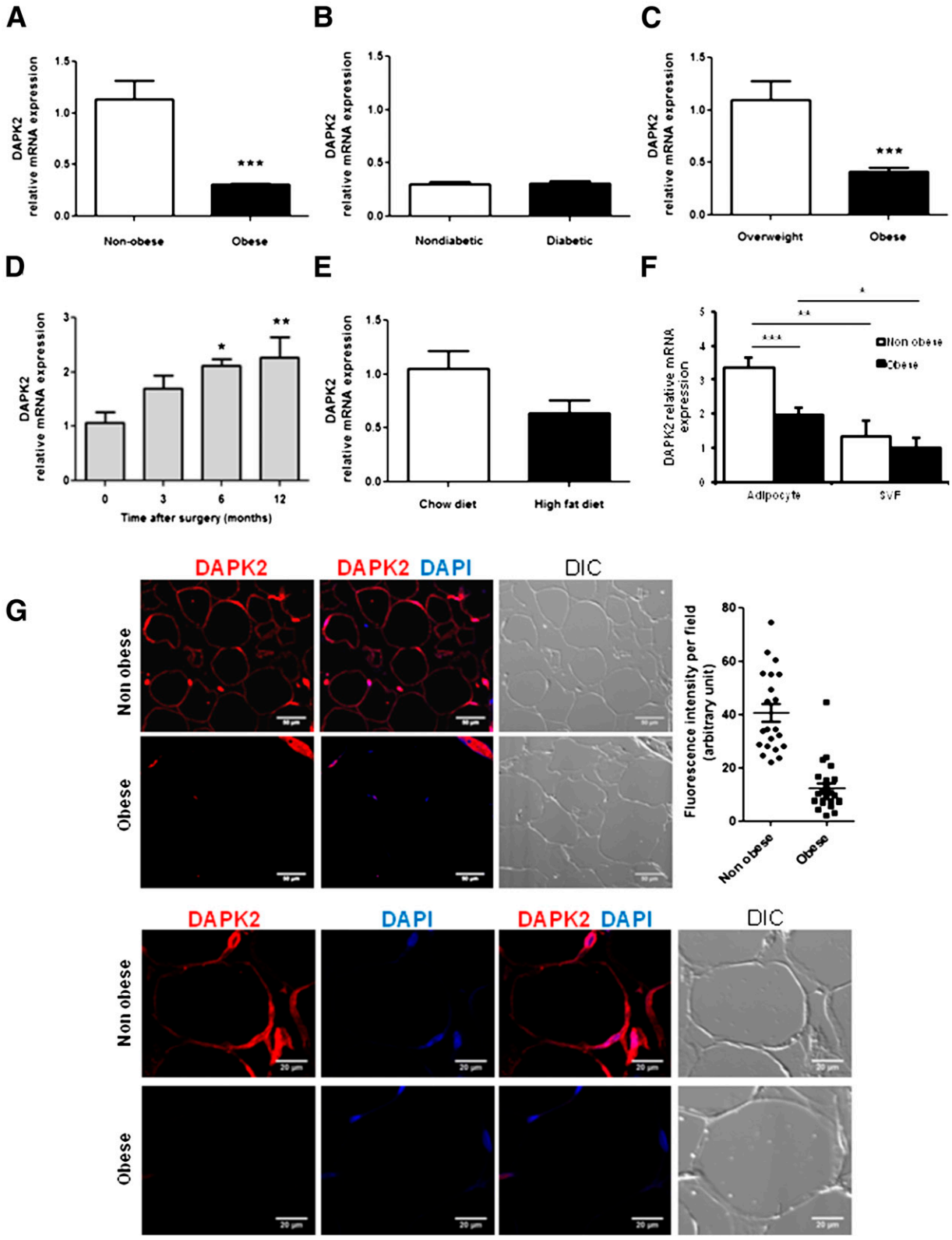

Figure 1—Downregulation of adipocyte DAPK2 expression in obesity. *A*: DAPK2 mRNA (relative to 18S) was quantified by RT-PCR in subcutaneous adipose tissue of 10 nonobese healthy subjects (mean BMI 23 kg/m^2) and 65 massively obese patients (BMI range 34–79 kg/m^2). *B*: Stratification of the obese group for diabetes (33 subjects among 65). *C*: DAPK2 mRNA in a subgroup of subjects with overweight (n = 10, BMI range 25–28 kg/m^2) or with massive obesity (n = 24). *D*: Time course of DAPK2 mRNA recovery after obesity treatment by gastric bypass surgery. Nine patients undergoing surgery were followed up over time, and adipose tissue specimens were collected. Significant changes before vs. after surgery were assessed by the Wilcoxon signed rank test. *E*: DAPK2 mRNA expression in inguinal adipose tissue of mice fed a control chow diet or high-fat diet for 16 weeks. Bars are mean ± SEM values from five individual mice.

Table 2—Association of adipose tissue DAPK2 mRNA expression with clinical parameters in obese patients

	Spearman coefficient	*P* value
Presurgery evaluation		
Triglyceridemia	−0.36216	0.0056
Serum IL-6	−0.28225	0.0448
Subcutaneous fat cell surface	−0.24069	0.0574
HDL cholesterol	0.35756	0.0063
12-month postsurgery evaluation		
Glycemia	−0.69007	0.0397

also detectable as LC3-II fast-migrating bands on Western blots (Fig. 2*B*), which accumulated in the presence of lysosomal inhibitors such as chloroquine, leupeptin/NH_4Cl, or bafilomycin A1, indicating ongoing autophagic clearance. As expected, nutrient withdrawal from culture medium increased autophagy flux (Fig. 2*C*) in agreement with well-known induction of autophagy by cell starvation. In some cell types, such as hepatocytes (25) or macrophages (26), intracellular lipid droplet organelles can end up in lysosomes for lipid degradation through so-called lipophagy. Lipophagy is poorly documented in fat cells, but the importance of activation of cytoplasmic neutral lipases for lipid droplet degradation is clearly established (27). We observed no increase in autophagic flux during acute lipolytic stimulation of 3T3-L1 adipocytes with the β-adrenergic agonist isoproterenol (Fig. 2*D*), and lysosomal inhibitors only marginally affected lipid mobilization as judged by cell glycerol release into the medium (Fig. 2*E*). Thus, autophagic clearance and lipid store mobilization by catecholamines are distinct processes in adipocytes.

DAPK2 mRNA expression in terminally differentiated 3T3-L1 adipocytes was two orders of magnitude lower than the two other related DAPKs (Fig. 3*A*), pointing to the 3T3-L1 model as a suitable system to explore the effect of exogenous DAPK2. Adenoviral (Ad)-based expression of DAPK2 (Ad-DAPK2) or a kinase-dead mutant version (Ad-DAPK2-K52A), coexpressed with an EGFP reporter, indicated a high proportion of transduced fat cells after 24 h (not shown). Compared with cells transduced with a null virus, DAPK2 expression did not produce overt metabolic effects. Cells continued to respond to acute insulin stimulation by massive Akt phosphorylation (Fig. 3*B*) and still contained lipid droplets with normal size distribution (Fig. 3*C*). Metabolic (leptin, adiponectin, fatty acid synthase, or perilipin 1) and inflammatory (IL-6, chemokine [C-C motif] ligand-2) gene expression was also unaltered (Fig. 3*D*). Furthermore, we observed no sign of cell leakage by cytoplasmic lactate dehydrogenase release (Fig. 3*E*), indicating unaffected cell viability. Considering a trend (+20%) toward increased ability to release glycerol upon adrenergic lipolytic stimulation (Fig. 3*F*), DAPK2-expressing adipocytes showed no evidence for dysfunction or death. Adipocyte clearance by autophagy (i.e., autophagic flux), as measured by LC3-II accumulation in the presence of lysosomal inhibitors, was higher in cells expressing DAPK2 than in cells transduced with viral backbone alone (Fig. 3*G*). Furthermore, DAPK2-mediated stimulation of autophagic clearance was abolished with a kinase-dead mutant version, indicating dependence on kinase activity for autophagy modulation (Fig. 3*H*).

We next evaluated the effect of DAPK2 inhibition by siRNA in human preadipocytes obtained from adipose tissue SVF. siRNA sequences decreased DAPK2 protein by half (Fig. 4*A*), increased cell contents of the p62 autophagic substrate (Fig. 4B), and decreased autophagosome accumulation with lysosome inhibitors, indicating reduced autophagic flux (Fig. 4*C*). All together, these data on gain or loss of function demonstrate that modulation of DAPK2 expression in adipose cells associates with basal autophagic tone regulation.

Adipocyte Autophagic Clearance Is Impaired in Obesity and Partially Reversed After Weight Loss

The above results suggest that downregulated adipocyte DAPK2 might be linked to attenuation of autophagic clearance in obesity. We therefore prepared isolated adipocyte cell fractions from obese and lean subcutaneous fat biopsy specimens and evaluated steady-state levels of the autophagic substrate p62, which were elevated twofold in obese versus lean adipocytes (Fig. 5*A* and *B*), indicative of lower autophagic degradation. Nevertheless, p62 mRNA was also higher in adipocytes from obese subjects compared with control subjects (Fig. 5*C*), precluding any definite conclusion on autophagic flux based on p62 protein content. We next set up an experiment in which freshly isolated adipocytes were incubated in a standard nutrient-rich medium, in the presence or absence of lysosome inhibitors, to evaluate rates of autophagosome accumulation (i.e., adipocyte autophagic flux). LC3-II accumulation in the presence of lysosome inhibitors was obvious in nonobese adipocytes but was only barely detected in obese fat cells (Fig. 5*D*). Quantitative analysis of LC3-II accumulation rates demonstrated reduced adipocyte autophagic clearance in obesity (Fig. 5E). Furthermore,

F: Floating adipocyte fraction was separated from the SVF by collagenase digestion of adipose tissue specimens obtained from 9 lean and 10 obese subjects. DAPK2 expression (relative to 18S) was determined in paired cell fractions by quantitative RT-PCR. Statistically significant differences between groups are indicated. ***$P < 0.001$; **$P < 0.01$; *$P < 0.05$. *G*: DAPK2 immunolabeling of subcutaneous adipose tissue sections. DAPK2 fluorescence intensity was quantified using ImageJ software, and background values obtained by omitting primary antibody were subtracted. A total of 50 adipose tissue fields from three lean and three obese donors were quantified. DIC, differential interference contrast.

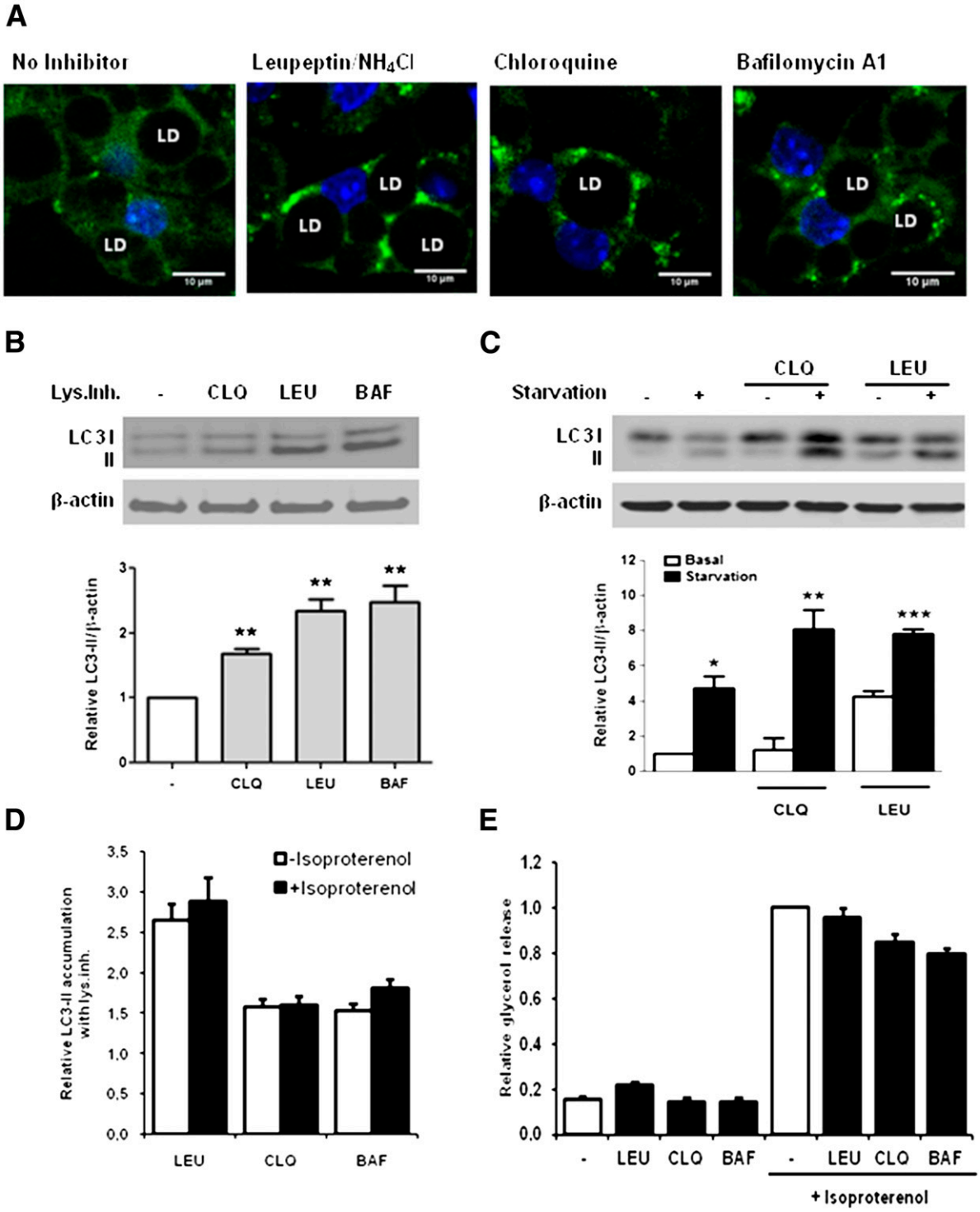

Figure 2—Constitutive lysosome-mediated autophagy in cultured adipocytes. *A*: Terminally differentiated 3T3-L1 stably expressing GFP-LC3. Growing 3T3-L1 cells were transfected with a retroviral pBabe construct expressing GFP-LC3, and stably expressing cells were selected with puromycin. Differentiation was induced under standard conditions. Terminally differentiated cells (day 12) were left untreated (basal) or incubated for 2 h with indicated lysosome inhibitors chloroquine (CLQ), leupeptin/NH_4Cl (LEU), or bafilomycin A1 (BAF) in serum-containing medium. Confocal fluorescent images are shown after fixation and DAPI staining of nuclei. Circular black areas in cells are lipid droplets (LD). *B*: Terminally differentiated 3T3-L1 were treated or not with lysosomal inhibitors (Lys.Inh.) as in *A* and lysed for LC3 analysis by Western blotting. Bars represent inhibitor-induced accumulation of LC3-II/actin relative to medium with no inhibitor. Values are mean ± SEM from 10 independent experiments. *C*: 3T3-L1 adipocytes were incubated for 1 h with Hanks' Balanced Salt Solution (starvation) or complete medium. *D* and *E*: 3T3-L1 adipocytes lipolytic stimulation by isoproterenol (10^5 mol/L, 2 h) in the presence of lysosomal inhibitors. Values are mean ± SEM in six experiments. *D*: LC3-II accumulation as in *C*. *E*: Glycerol release into the medium was expressed as nmol/mg cell protein. Values obtained in isoproterenol-stimulated cells with no inhibitor were set to 1. Asterisks indicate statistical significance for *P* values: $^*P < 0.05$, $^{**}P < 0.01$, or $^{***}P < 0.001$.

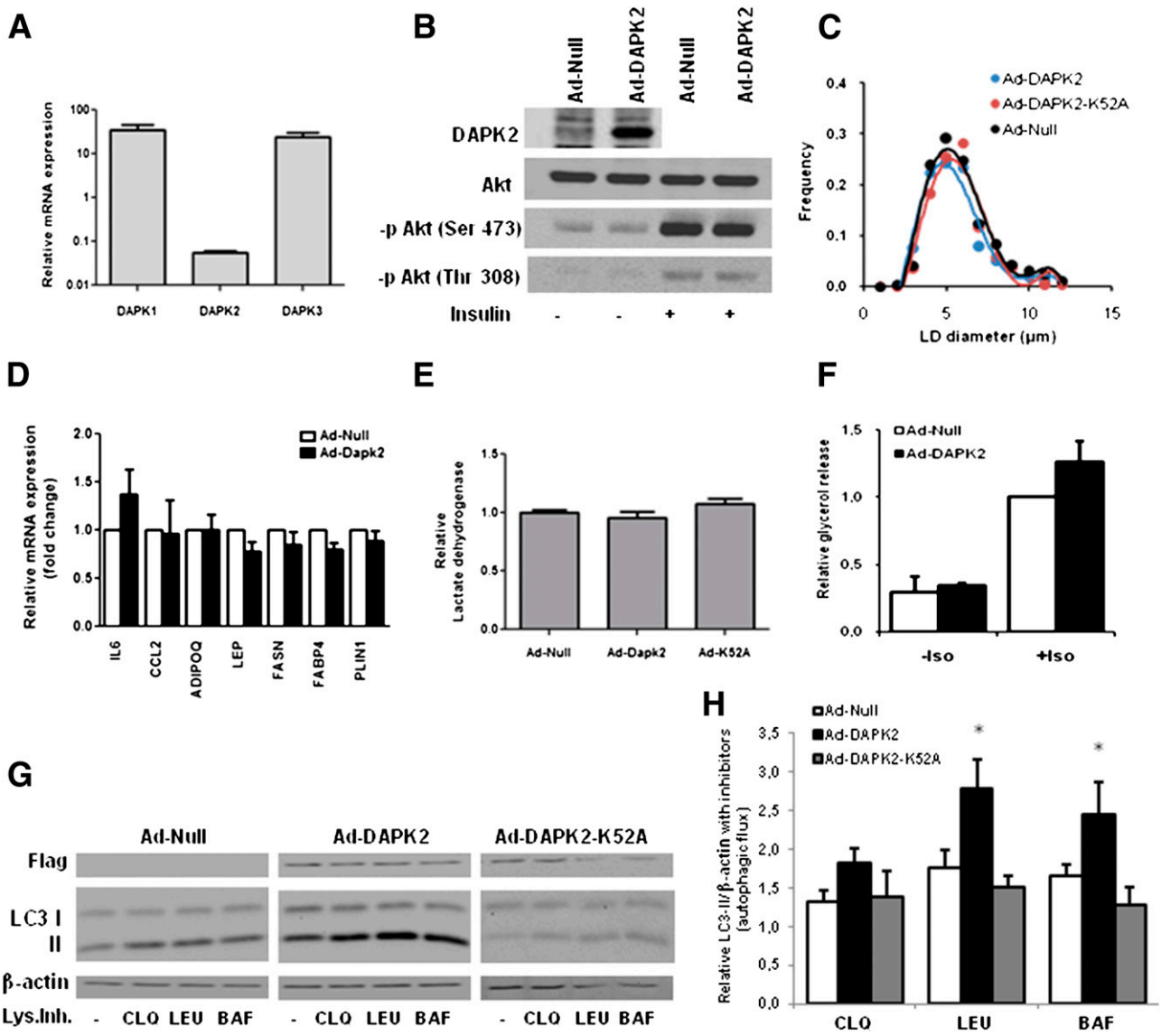

Figure 3—DAPK2 exogenous expression increases adipocyte autophagic clearance in 3T3-L1. *A*: Relative expression of the three DAPKs in terminally differentiated 3T3-L1 adipocytes. Expression is normalized to 18S RNA. At least three independent mRNA preparations were used for quantification. *B*: Insulin response in Ad-DAPK2–expressing 3T3-L1 cells. Terminally differentiated cells were transduced with indicated adenoviruses and left in standard medium for 24 h (in the absence of insulin). Stimulation with the hormone was for 15 min with 100 nmol/L in DMEM. DAPK2 and Akt were assessed on separate membranes using lysates from the same cell batches. Phosphorylation of Akt (-p Akt) on indicated amino acid residues was probed with phosphorylation-specific antibodies. *C*: At 24 h after virus transduction, terminally differentiated cells were imaged by phase contrast to measure lipid droplet (LD) size using Perfect Image software. Four images from random fields were quantified, representing >500 individual LDs in each group. LD size distributions in a representative experiment are shown. *D*: Differentiated 3T3-L1 cells were transduced with adenovirus and used for mRNA extraction after 24 h. Indicated mRNA were measured by RT-PCR, normalized to 18S mRNA, and expressed relative to the control group. RNA was obtained from at least three independent experiments. *E*: Lactate dehydrogenase release into the medium was assessed 24 h after adenovirus transduction. A representative experiment of two is shown. *F*: Lipolytic activity of terminally differentiated 3T3-L1, 24 h after transduction with indicated adenoviruses. Glycerol release into the medium was measured and normalized to cell protein content. Values for maximal isoproterenol (Iso) stimulation are set to 1, bars are means from two independent experiments. *G*: Cells expressing DAPK2 or a kinase-dead mutant version were incubated in complete medium for 2 h in the presence or absence or lysosomal inhibitors (Lys.Inh.) and lysed for Western blot analysis. *H*: Autophagic flux quantification. LC3-II/actin accumulation in the presence (vs. absence) of lysosome inhibitors is calculated from five independent experiments. BAF, bafilomycin A1; CLQ, chloroquine; LEU, leupeptin/NH_4Cl. *$P < 0.05$ indicating a statistically significant difference.

adipocyte autophagic flux inversely correlated with fat cell size (Fig. 5*F*), which is primarily determined by lipid amounts within the unilocular lipid droplet. Thus, attenuated autophagic flux in obesity is linked with adipocyte lipid overload. Similarly, adipocytes isolated from obese (*ob*/*ob*) mice also exhibited lower autophagic activity than nonobese (*ob*/+) controls (Fig. 5*G* and *H*), indicating common reduction in obese rodents and humans.

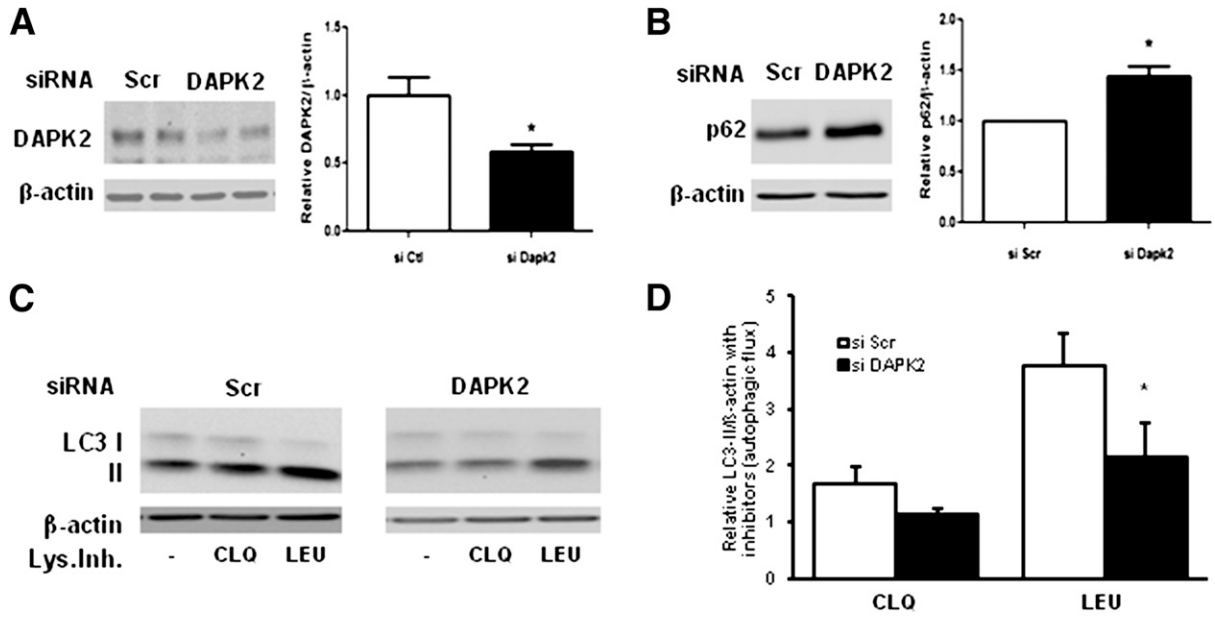

Figure 4—siRNA-mediated DAPK2 inhibition reduces autophagic flux. Effect of DAPK2 inhibition by siRNA on endogenous DAPK2 (*A*) and p62 (*B*) content. Control cells were transfected with scrambled (Scr) siRNA. *C*: Cells were incubated in complete serum-supplemented medium for 2 h in the presence or absence of lysosome inhibitors and lysed for Western blot analysis. *D*: Bars represent quantification of LC3-II accumulation with lysosome inhibitors (Lys.Inh.) (autophagic flux) as mean values ± SEM of three independent experiments with different cell donors in which LC3-II/actin signals with no inhibitor were arbitrarily set to 1. CLQ, chloroquine; Ctl, control; LEU, leupeptin/NH_4Cl. *$P < 0.05$ indicating statistical significance.

Reversibility of autophagy attenuation was investigated by assessing adipocyte preparations obtained from obese patients after bariatric surgery–induced weight loss. In nine patients, adipose tissue samples were obtained pre- and postsurgery at one occasion within 3 to 12 months after the intervention. All patients lost weight and reduced subcutaneous adipocyte cell size and lipid contents (Fig. 6*A*), although at different degrees, because of the large time frame in postsurgery sample collection. Interestingly, total adipocyte LC3 protein content pre- versus postsurgery changed proportionally to the extent of adipocyte size reduction (Fig. 6B). Pre- versus postsurgery comparisons indicated ameliorated adipocyte autophagic clearance in all patients (Fig. 6*C*) and significant recovery, regardless of the use of chloroquine or leupeptin to evaluate autophagic flux (Fig. 6*D* and *E*). Thus, adipocyte lysosome–mediated remodeling is compromised in obesity, and partial recovery can be obtained by weight loss.

DISCUSSION

Increasing evidence points to the critical role of autophagy in metabolic diseases, linked to the adaptive response to chronic metabolic stress (28). In almost every tissue participating in energy homeostasis (liver, pancreas, muscle, and even hypothalamus), invalidation of autophagy by tissue-specific gene knockout was found to be associated with metabolic dysfunction (25,29–33). However, adipocyte responses are still poorly understood because invalidation of adenine thymine guanine alters normal fat tissue differentiation (34,35). Our study brings new evidence that autophagy attenuation associates with adipocyte dysfunction in obesity. Interestingly, previous reports showed autophagy activation in adipose tissue in human or mice obesity (36–38). Noteworthy, the study of total adipose tissue takes account of obesity-associated inflammatory cells, in which autophagy is linked to immune function, so that it remains unclear from these reports in which cell type autophagy is modulated. Here, specific focus on adipocytes and direct measurement of autophagosome clearance show that obesity is associated with downregulation of adipocyte autophagic turnover, partially recovering after bypass surgery–mediated weight loss. Our data are in line with a negative role of lipids on autophagosome dynamics (39,40) and with high-fat diet–induced autophagy defects previously demonstrated in the liver (41,42), kidney (43), and hypothalamus (44).

Autophagic degradation of lipid droplets, also called lipophagy, can decrease the intracellular lipid burden in many cell types but is shown here to only marginally modulate in vitro adipocyte lipolysis. This is in good agreement with the prominent role of neutral cytoplasmic lipases in fat cell lipid mobilization (27) and suggests that autophagy might control other adipocyte phenotypes. Indeed, autophagy inhibition potently induces cell inflammation (45), including fat cell inflammation (37,46). Furthermore, mice with systemic haploinsufficiency for the Atg7 autophagy gene overproduce reactive oxygen species in adipose tissue when obese (47). Thus, we favor the possibility that autophagy serves in the long-term to dampen adipocyte inflammation linked to metabolic dysfunctions.

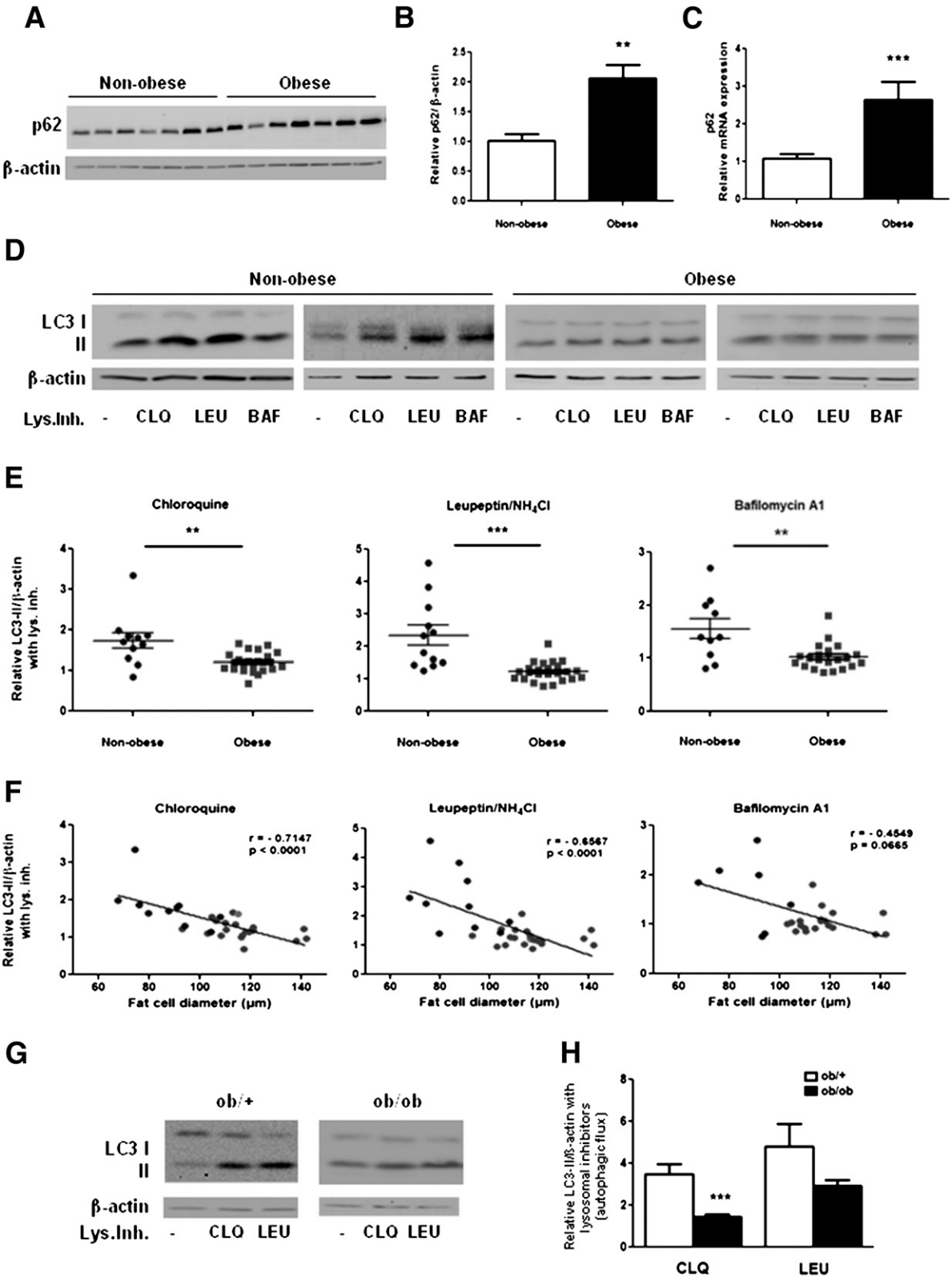

Figure 5—Decreased adipocyte autophagic clearance in human and rodent obesity. *A*: Freshly isolated adipocytes obtained by collagenase digestion of 24 obese patients and 12 nonobese control patients were lysed and proteins (15 μg) analyzed by Western blotting. *B*: A representative blot is shown with quantitative analysis of p62. *C*: p62 mRNA quantification by RT-PCR performed on adipocyte RNA preparation (10 nonobese and 14 obese patients). Values were normalized to 18S. Bars are means ± SEM of signal intensity relative to values of nonobese control subjects set to 1. *D* and *E*: Autophagic flux in adipocytes freshly obtained from adipose tissue biopsies as in *A*. Adipocytes were incubated in DMEM medium for 2 h, with or without lysosomal inhibitors (Lys.Inh.), as indicated (chloroquine [CLQ], leupeptin/NH_4Cl [LEU], bafilomycin A1 [BAF]). *E*: Each point represents inhibitor-induced LC3-II accumulation relative to LC3 content with

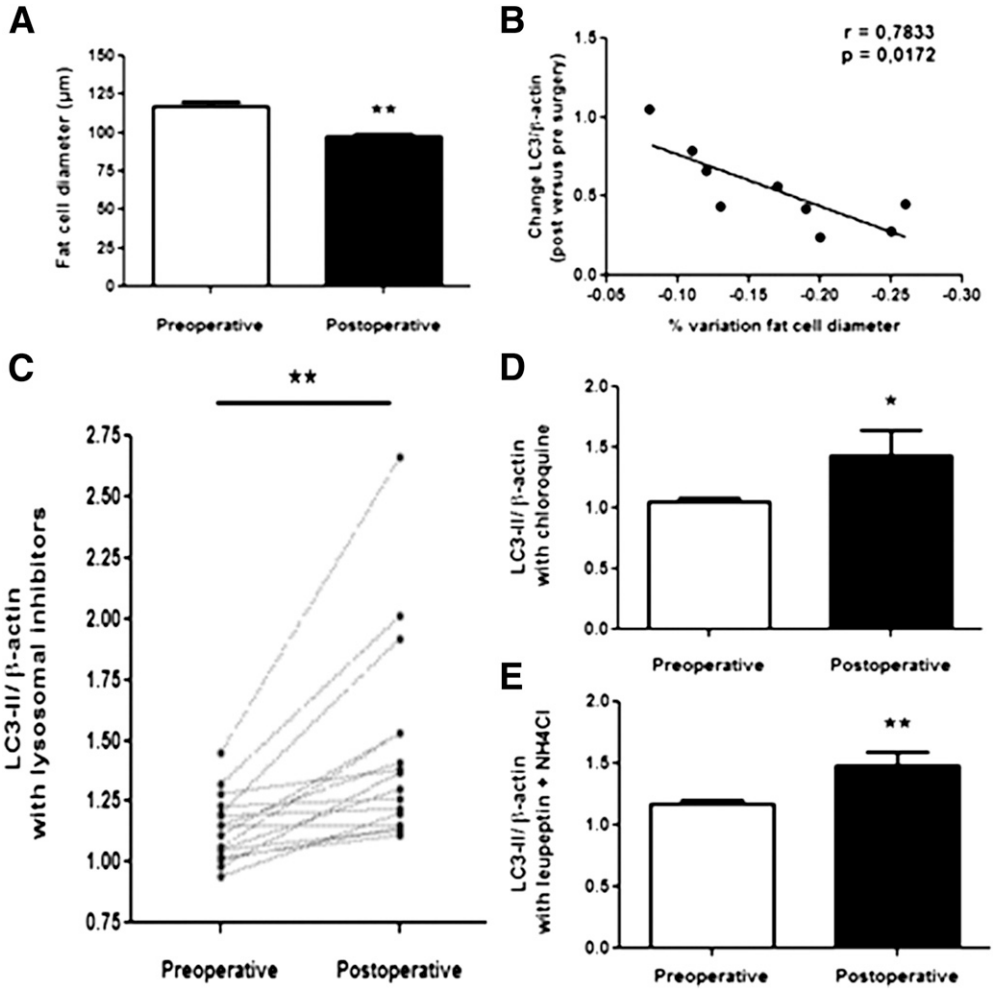

Figure 6—Recovery of autophagy by weight loss after bariatric surgery. Adipose tissue needle biopsies were obtained from nine obese patients before and after surgery (once after intervention, within 3 to 12 months). *A*: Adipocytes were isolated from the biopsy specimens and used to determine adipocyte size. *B*: Spearman correlation between change in LC3 expression and fat cell size reduction after surgery. *C–E*: Changes in adipocyte autophagic flux after surgery. Data obtained in individual cell preparations irrespective of lysosomal inhibitor are plotted in *C*. Mean values ± SEM of pre- vs. postsurgery autophagic flux evaluated with chloroquine or leupeptin/NH_4Cl are shown in *D* and *E*. Asterisks indicate statistical significance for *P* values: $^*P < 0.05$; $^{**}P < 0.01$.

The current study links obesity-related downregulation of a kinase, DAPK2, with attenuation of adipocyte autophagy. DAPK2 was reported proapoptotic when transiently overexpressed (48,49). In the context of adipose cells lines with low endogenous expression, we found no evidence for cell death induction after Ad-mediated DAPK2 protein expression. Furthermore, by retroviral-mediated gene transfer, we could obtain viable 3T3-L1 adipocyte clones stably expressing wild-type DAPK2 but not the constitutively active form. Thus, we believe that DAPK2 is not proapoptotic in the adipocyte cell environment, likely because of fine-tuning of kinase activation by appropriate mechanisms. Our present data, rather, indicate that DAPK2 is linked to constitutive autophagy and provide evidence that kinase activity is required for this regulation. Molecular mechanisms by which DAPK2 sustains autophagic clearance are not yet elucidated but might involve the targeting of autophagy proteins still to be defined. Recently, several DAPK2 interacting partners or substrates have been identified in the autophagy protein network, including inhibitory interaction with 14-3-3, interference with mammalian target of rapamycin complex inhibition, or participation in

no inhibitor. *F*: Spearman correlation between autophagic flux and adipocyte diameter. *G* and *H*: LC3-II/actin signals in adipocytes isolated from lean (*ob*/+) or obese (*ob*/*ob*) mice epididymal adipose tissue incubated with or without lysosome inhibitors. *G*: Representative blots from individual mice of each genotype are shown (six mice in each group were studied). *H*: Bars represent quantifications of autophagic flux (i.e., LC3-II/actin accumulation) in the presence vs. absence of lysosome inhibitor as mean values ± SEM. Asterisks indicate statistical significance for *P* values: $^*P < 0.05$, $^{**}P < 0.01$, or $^{***}P < 0.001$.

the beclin interactome (50,51). Interestingly, DAPK2 silencing was also found to affect tumor necrosis factor–related apoptosis-inducing ligand signaling and nuclear factor-κB activation (52), reinforcing connections to cell inflammation. Clearly, more understanding is needed before a unified view on DAPK2 molecular action emerges, but in the context of obesity-related meta-inflammation, our present data identify the loss of DAPK2 expression and establish a link to attenuated autophagic clearance of adipocytes, revealing a potential novel actor in metabolic diseases.

Acknowledgments. The authors thank A. Kimchi (Weizmann Institute of Science, Rehovot, Israel) for providing bacterial clones containing human DAPK2 cDNA sequences and K52A kinase-dead mutant version, Xavier Le Liepvre and Francoise Lasnier (INSERM, Paris, France) for virus construction, Joan Tordjman (UMR_S 1166, Paris, France) for providing paraffin-embedded adipose tissue sections, and Jean-Luc Bouillot (Ambroise Paré Hospital, Assistance Publique-Hôpitaux de Paris, Paris, France) for providing adipose tissue biopsies.

Funding. Financial support from Cardiovasculaire Obésité Rein Diabète (CORDDIM, Ile de France region) to H.S., from Clinical Research Program (PHRC 02076 on "adiposity signals") to K.C., and from The French National Research Agency (ANR-14CE12-0017-02 LIPOCAMD) to I.D. is acknowledged.

Duality of Interest. No potential conflicts of interest relevant to this article were reported.

Author Contributions. H.S., S.R., R.A., C.P., S.M., M.P., and C.R. performed experiments. H.S., K.C., and I.D. designed the study and wrote the manuscript. I.D. is the guarantor of this work and, as such, had full access to all the data in the study and takes responsibility for the integrity of the data and the accuracy of the data analysis.

References

1. Rosen ED, Spiegelman BM. What we talk about when we talk about fat. Cell 2014;156:20–44
2. Soukas A, Cohen P, Socci ND, Friedman JM. Leptin-specific patterns of gene expression in white adipose tissue. Genes Dev 2000;14:963–980
3. Weisberg SP, McCann D, Desai M, Rosenbaum M, Leibel RL, Ferrante AW Jr. Obesity is associated with macrophage accumulation in adipose tissue. J Clin Invest 2003;112:1796–1808
4. Clément K, Viguerie N, Poitou C, et al. Weight loss regulates inflammation-related genes in white adipose tissue of obese subjects. FASEB J 2004;18:1657–1669
5. Schipper HS, Prakken B, Kalkhoven E, Boes M. Adipose tissue-resident immune cells: key players in immunometabolism. Trends Endocrinol Metab 2012;23:407–415
6. Lumeng CN, Saltiel AR. Inflammatory links between obesity and metabolic disease. J Clin Invest 2011;121:2111–2117
7. Henegar C, Tordjman J, Achard V, et al. Adipose tissue transcriptomic signature highlights the pathological relevance of extracellular matrix in human obesity. Genome Biol 2008;9:R14
8. Deiss LP, Feinstein E, Berissi H, Cohen O, Kimchi A. Identification of a novel serine/threonine kinase and a novel 15-kD protein as potential mediators of the gamma interferon-induced cell death. Genes Dev 1995;9:15–30
9. Bialik S, Kimchi A. The death-associated protein kinases: structure, function, and beyond. Annu Rev Biochem 2006;75:189–210
10. Szyniarowski P, Corcelle-Termeau E, Farkas T, et al. A comprehensive siRNA screen for kinases that suppress macroautophagy in optimal growth conditions. Autophagy 2011;7:892–903
11. Farhan H, Wendeler MW, Mitrovic S, et al. MAPK signaling to the early secretory pathway revealed by kinase/phosphatase functional screening. J Cell Biol 2010;189:997–1011
12. Barrios-Rodiles M, Brown KR, Ozdamar B, et al. High-throughput mapping of a dynamic signaling network in mammalian cells. Science 2005;307:1621–1625
13. Rodbell M. Metabolism of isolated fat cells. I: effects of hormones on glucose metabolism and lipolysis. J Biol Chem 1964;239:375–380
14. Logette E, Le Jossic-Corcos C, Masson D, et al. Caspase-2, a novel lipid sensor under the control of sterol regulatory element binding protein 2. Mol Cell Biol 2005;25:9621–9631
15. Briand N, Prado C, Mabilleau G, et al. Caveolin-1 expression and cavins stability regulate caveolae dynamics in adipocyte lipid store fluctuation. Diabetes 2014;63:4032–4044
16. Toubal A, Clément K, Fan R, et al. SMRT-GPS2 corepressor pathway dysregulation coincides with obesity-linked adipocyte inflammation. J Clin Invest 2013;123:362–379
17. Klionsky DJ, Abdalla FC, Abeliovich H, et al. Guidelines for the use and interpretation of assays for monitoring autophagy. Autophagy 2012;8:445–544
18. Le Lay S, Briand N, Blouin CM, et al. The lipoatrophic caveolin-1 deficient mouse model reveals autophagy in mature adipocytes. Autophagy 2010;6:754–763
19. Tondu AL, Robichon C, Yvan-Charvet L, et al. Insulin and angiotensin II induce the translocation of scavenger receptor class B, type I from intracellular sites to the plasma membrane of adipocytes. J Biol Chem 2005;280:33536–33540
20. Briand N, Le Lay S, Sessa WC, Ferré P, Dugail I. Distinct roles of endothelial and adipocyte caveolin-1 in macrophage infiltration and adipose tissue metabolic activity. Diabetes 2011;60:448–453
21. Spalding KL, Arner E, Westermark PO, et al. Dynamics of fat cell turnover in humans. Nature 2008;453:783–787
22. Boya P, Reggiori F, Codogno P. Emerging regulation and functions of autophagy. Nat Cell Biol 2013;15:713–720
23. Jegga AG, Schneider L, Ouyang X, Zhang J. Systems biology of the autophagy-lysosomal pathway. Autophagy 2011;7:477–489
24. Inbal B, Bialik S, Sabanay I, Shani G, Kimchi A. DAP kinase and DRP-1 mediate membrane blebbing and the formation of autophagic vesicles during programmed cell death. J Cell Biol 2002;157:455–468
25. Singh R, Kaushik S, Wang Y, et al. Autophagy regulates lipid metabolism. Nature 2009;458:1131–1135
26. Ouimet M, Franklin V, Mak E, Liao X, Tabas I, Marcel YL. Autophagy regulates cholesterol efflux from macrophage foam cells via lysosomal acid lipase. Cell Metab 2011;13:655–667
27. Young SG, Zechner R. Biochemistry and pathophysiology of intravascular and intracellular lipolysis. Genes Dev 2013;27:459–484
28. Kroemer G, Mariño G, Levine B. Autophagy and the integrated stress response. Mol Cell 2010;40:280–293
29. Jung HS, Chung KW, Won Kim J, et al. Loss of autophagy diminishes pancreatic beta cell mass and function with resultant hyperglycemia. Cell Metab 2008;8:318–324
30. Razani B, Feng C, Coleman T, et al. Autophagy links inflammasomes to atherosclerotic progression. Cell Metab 2012;15:534–544
31. He C, Bassik MC, Moresi V, et al. Exercise-induced BCL2-regulated autophagy is required for muscle glucose homeostasis. Nature 2012;481:511–515
32. Coupé B, Ishii Y, Dietrich MO, Komatsu M, Horvath TL, Bouret SG. Loss of autophagy in pro-opiomelanocortin neurons perturbs axon growth and causes metabolic dysregulation. Cell Metab 2012;15:247–255
33. Baerga R, Zhang Y, Chen PH, Goldman S, Jin S. Targeted deletion of autophagy-related 5 (atg5) impairs adipogenesis in a cellular model and in mice. Autophagy 2009;5:1118–1130

34. Singh R, Xiang Y, Wang Y, et al. Autophagy regulates adipose mass and differentiation in mice. J Clin Invest 2009;119:3329–3339
35. Zhang Y, Goldman S, Baerga R, Zhao Y, Komatsu M, Jin S. Adipose-specific deletion of autophagy-related gene 7 (atg7) in mice reveals a role in adipogenesis. Proc Natl Acad Sci U S A 2009;106:19860–19865
36. Kovsan J, Blüher M, Tarnovscki T, et al. Altered autophagy in human adipose tissues in obesity. J Clin Endocrinol Metab 2011;96:E268–E277
37. Jansen HJ, van Essen P, Koenen T, et al. Autophagy activity is up-regulated in adipose tissue of obese individuals and modulates proinflammatory cytokine expression. Endocrinology 2012;153:5866–5874
38. Nuñez CE, Rodrigues VS, Gomes FS, et al. Defective regulation of adipose tissue autophagy in obesity. Int J Obes (Lond) 2013;37:1473–1480
39. Koga H, Kaushik S, Cuervo AM. Altered lipid content inhibits autophagic vesicular fusion. FASEB J 2010;24:3052–3065
40. Las G, Serada SB, Wikstrom JD, Twig G, Shirihai OS. Fatty acids suppress autophagic turnover in β-cells. J Biol Chem 2011;286:42534–42544
41. Liu HY, Han J, Cao SY, et al. Hepatic autophagy is suppressed in the presence of insulin resistance and hyperinsulinemia: inhibition of FoxO1-dependent expression of key autophagy genes by insulin. J Biol Chem 2009;284:31484–31492
42. Yang L, Li P, Fu S, Calay ES, Hotamisligil GS. Defective hepatic autophagy in obesity promotes ER stress and causes insulin resistance. Cell Metab 2010;11:467–478
43. Yamahara K, Kume S, Koya D, et al. Obesity-mediated autophagy insufficiency exacerbates proteinuria-induced tubulointerstitial lesions. J Am Soc Nephrol 2013;24:1769–1781
44. Meng Q, Cai D. Defective hypothalamic autophagy directs the central pathogenesis of obesity via the IkappaB kinase beta (IKKbeta)/NF-kappaB pathway. J Biol Chem 2011;286:32324–32332
45. Deretic V, Saitoh T, Akira S. Autophagy in infection, inflammation and immunity. Nat Rev Immunol 2013;13:722–737
46. Yoshizaki T, Kusunoki C, Kondo M, et al. Autophagy regulates inflammation in adipocytes. Biochem Biophys Res Commun 2012;417:352–357
47. Lim YM, Lim H, Hur KY, et al. Systemic autophagy insufficiency compromises adaptation to metabolic stress and facilitates progression from obesity to diabetes. Nat Commun 2014;5:4934
48. Kawai T, Nomura F, Hoshino K, et al. Death-associated protein kinase 2 is a new calcium/calmodulin-dependent protein kinase that signals apoptosis through its catalytic activity. Oncogene 1999;18:3471–3480
49. Inbal B, Shani G, Cohen O, Kissil JL, Kimchi A. Death-associated protein kinase-related protein 1, a novel serine/threonine kinase involved in apoptosis. Mol Cell Biol 2000;20:1044–1054
50. Gilad Y, Shiloh R, Ber Y, Bialik S, Kimchi A. Discovering protein-protein interactions within the programmed cell death network using a protein-fragment complementation screen. Cell Reports 2014;8:909–921
51. Ber Y, Shiloh R, Gilad Y, Degani N, Bialik S, Kimchi A. DAPK2 is a novel regulator of mTORC1 activity and autophagy. Cell Death Differ 2014;22:465–475
52. Schlegel CR, Fonseca AV, Stöcker S, et al. DAPK2 is a novel modulator of TRAIL-induced apoptosis. Cell Death Differ 2014;21:1780–1791